

A Bayesian Framework for Multivariate Differential Analysis accounting for Missing Data

Marie Chion^{1*} & Arthur Leroy²

¹ MRC Biostatistics Unit, University of Cambridge, United Kingdom.

² Department of Computer Science, The University of Manchester, United Kingdom.

* Corresponding author: marie.chion@protonmail.com

Abstract

Current statistical methods in differential proteomics analysis generally leave aside several challenges, such as missing values, correlations between peptides' intensities and uncertainty quantification. Moreover, they provide point estimates, such as the mean intensity for a given peptide or protein in a given condition. The decision whether an analyte should be considered as *differential* is then based on comparing the p-value to a significance threshold, usually 5%. In the state-of-the-art `limma` approach, a hierarchical model is used to deduce the posterior distribution of the variance estimator for each analyte. The expectation of this distribution is then used as a moderated estimation of variance and is injected directly into the expression of the t-statistic. However, instead of merely relying on the moderated estimates, we could provide more powerful and intuitive results by leveraging a fully Bayesian approach and hence allow the quantification of uncertainty. The present work introduces this idea by taking advantage of standard results from Bayesian inference with conjugate priors in hierarchical models to derive a methodology tailored to handle multiple imputation contexts. Furthermore, we aim to tackle the more general problem of multivariate differential analysis, to account for possible inter-peptide correlations. By defining a hierarchical model with prior distributions on both mean and variance parameters, we achieve a global quantification of the uncertainty for differential analysis. The inference is thus performed by computing the posterior distribution for the difference in mean peptide intensities between two experimental conditions. In contrast to more flexible models that can be achieved with hierarchical structures, our choice of conjugate priors maintains analytical expressions for direct sampling from posterior distributions without requiring expensive MCMC methods. The performances of this approach have been assessed through extensive simulation studies as well as application to a real-world controlled dataset. We demonstrated its ability to provide more accurate and intuitive results than standard t-tests for handling differential analysis in proteomics.

1 Introduction

Context. Differential proteomics analysis aims to compare peptide and/or protein expression levels across several biological conditions. The massive data provided by label-free mass spectrometry-based quantitative proteomics experiments requires reliable statistical modelling tools to assess which protein is differentially abundant. Table 1 shows the state-of-the-art tools for differential proteomics analysis. They are based on well-known statistical methods, yet they are faced with several challenges. First, they rely on complete datasets. However, quantitative proteomics data usually contains missing values. In label-free quantitative proteomics, missing value proportion ranges between 10% and 50% according to Lazar et al. (2016). Imputation remedies this problem by replacing a missing value with a user-defined one. In particular, multiple imputation (Little and Rubin, 2019) consists in generating several imputed datasets that are then combined in order to get an estimator of the parameter of interest (often the mean peptide or protein intensity in a given condition) and an estimator of its variability. Recent work from Chion et al. (2022) includes the uncertainty induced by the

Method	Software
t-tests	Perseus (Tyanova et al., 2016) DAPAR (Wieczorek et al., 2017) PANDA-view (Chang et al., 2018)
ANOVA	Perseus (Tyanova et al., 2016) PANDA-view (Chang et al., 2018)
Moderated t-test (limma)	DAPAR (Wieczorek et al., 2017) mi4p (Chion et al., 2022)
Linear model	MSstats (Choi et al., 2014) proDA (Ahlmann-Eltze and Anders, 2020)

Table 1: State-of-the-art software for differential proteomics analysis

multiple imputation process in the previously described moderated t -testing framework from Smyth (2004). This method relies on a hierarchical model used to deduce the posterior distribution of the variance estimator for each analyte. The expectation of this distribution is then used as a moderated estimation of variance and is injected directly into the expression of the t -statistic. However, instead of relying simply on the moderated estimates, taking advantage of a fully Bayesian approach could make sense. The topic of missing data has been under investigation in the Bayesian community for a long time, particularly in simple cases involving conjugate priors (Dominici et al., 2000). Despite such theoretical advances, practitioners in proteomics often still rely on old-fashioned tools, like t -tests, for conducting most differential analyses. Recently, some authors provided convenient approaches and associated implementations (Kruschke, 2013) for handling differential analysis problems with Bayesian inference. For instance, the R package BEST (standing for Bayesian Estimation Supersedes T-test) has widely contributed to the diffusion of those practices. Crook et al. (2022) reviewed the contributions of Bayesian statistics to proteomics data analysis. O’Brien et al. (2018) suggested a Bayesian selection model to mitigate the problem of missing values. The and Käll (2019) implemented in `Triqler` a probabilistic model that accounts for different sources of variability from identification and quantification to differential analysis.

Contribution. The present article follows a similar idea by taking advantage of standard results from Bayesian inference with conjugate priors in hierarchical models to derive a methodology tailored to handle our multiple imputation context. Furthermore, we aim to tackle the more general problem of multivariate differential analysis, to account for possible correlations between analytes. They often consider each analyte independently from the other ones. Hence, they do not take advantage of the possible correlations between peptides that belong to the same protein (for example). By defining a hierarchical model with prior distributions on both mean and variance parameters, we aim to provide an adequate quantification of the uncertainty for differential analysis. Inference is thus performed by computing the posterior distribution for the difference in mean peptide intensity between two experimental conditions. In contrast to more flexible models that can be achieved with hierarchical structures, our choice of conjugate priors maintains analytical expressions for directly sampling from posterior distributions without needing MCMC methods. This results in a fast inference procedure in practice.

Outline. The paper is organised as follows: Section 2.1 presents well-known results about Bayesian inference for Gaussian-inverse-gamma conjugated priors. Following analogous results for the multivariate case, Section 2.2 introduces a general Bayesian framework for evaluating mean differences in our differential proteomics context. Section 2.3 provides insights on the particular case where the considered analytes are uncorrelated. The proofs of these methodological developments can be found in Section 7. Section 3 evaluates the framework through a simulation study, illustrating hands-on examples on a real proteomics dataset and highlights the benefits of such a multivariate Bayesian framework for practitioners.

2 Modelling

2.1 Bayesian inference for Normal-Inverse-Gamma conjugated priors

Before deriving our complete workflow, let us recall some classical Bayesian inference results that will further serve our aim. We assume a generative model such as:

$$y = \mu + \varepsilon,$$

- $\mu \mid \sigma^2 \sim \mathcal{N}\left(\mu_0, \frac{1}{\lambda_0} \sigma^2\right)$ is the prior distribution over the mean,
- $\varepsilon \sim \mathcal{N}(0, \sigma^2)$ is the error term,
- $\sigma^2 \sim \Gamma^{-1}(\alpha_0, \beta_0)$ is the prior distribution over the variance,

with $\{\mu_0, \lambda_0, \alpha_0, \beta_0\}$ an arbitrary set of prior hyper-parameters. In Figure 1, we provide an illustration of the hypotheses taken over such a hierarchical generative model.

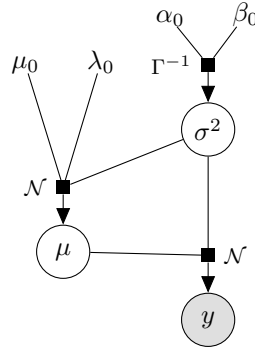


Figure 1: Graphical model of the hierarchical structure when assuming a Gaussian-inverse-gamma prior, conjugated with a Gaussian likelihood with unknown mean and variance.

From the previous hypotheses, we can deduce the likelihood of the model for a sample of observations $\mathbf{y} = \{y_1, \dots, y_N\}$:

$$\begin{aligned} p(\mathbf{y} \mid \mu, \sigma^2) &= \prod_{n=1}^N p(y_n \mid \mu, \sigma^2) \\ &= \prod_{n=1}^N \mathcal{N}(y_n; \mu, \sigma^2), \end{aligned}$$

Let us recall that such assumptions define a prior Gaussian-inverse-gamma distribution, which is conjugated with the Gaussian distribution with unknown mean μ and variance σ^2 . The probability density function (PDF) of such a prior distribution can be written as follows:

$$p(\mu, \sigma^2 \mid \mu_0, \lambda_0, \alpha_0, \beta_0) = \frac{\sqrt{\lambda_0}}{\sqrt{2\pi}} \frac{\beta_0^{\alpha_0}}{\Gamma(\alpha_0)} \left(\frac{1}{\sigma^2}\right)^{\alpha_0 + \frac{3}{2}} \exp\left(-\frac{2\beta_0 + \lambda_0(\mu - \mu_0)^2}{2\sigma^2}\right).$$

In this particular case, it is a well-known result that the inference is tractable and the posterior distribution remains a Gaussian-inverse-gamma (Murphy, 2007). The proof is available in section 7.1.

Therefore, the joint posterior distribution can be expressed as:

$$\mu, \sigma^2 \mid \mathbf{y} \sim \mathcal{N}\Gamma^{-1}(\mu_N, \lambda_N, \alpha_N, \beta_N) \quad (1)$$

with:

- $\mu_N = \frac{N\bar{y} + \lambda_0\mu_0}{\lambda_0 + N},$

- $\lambda_N = \lambda_0 + N$,
- $\alpha_N = \alpha_0 + \frac{N}{2}$,
- $\beta_N = \beta_0 + \frac{1}{2} \sum_{n=1}^N (y_n - \bar{y})^2 + \frac{\lambda_0 N}{2(\lambda_0 + N)} (\bar{y} - \mu_0)^2$.

Although these update formulas provide a valuable result, we shall see in the sequel that we are more interested in the marginal distribution over the mean parameter μ for comparison purposes. Computing this marginal from the joint posterior in Equation (1) remains tractable as well by integrating over σ^2 :

$$\begin{aligned}
p(\mu | \mathbf{y}) &= \int p(\mu, \sigma^2 | \mathbf{y}) d\sigma^2 \\
&= \frac{\sqrt{\lambda_N}}{\sqrt{2\pi}} \frac{\beta_N^{\alpha_N}}{\Gamma(\alpha_N)} \int \left(\frac{1}{\sigma^2}\right)^{\alpha_N + \frac{3}{2}} \exp\left(-\frac{2\beta_N + \lambda_N(\mu - \mu_N)^2}{2\sigma^2}\right) d\sigma^2 \\
&= \frac{\Gamma(\frac{\nu+1}{2})}{\Gamma(\frac{\nu}{2})} \frac{1}{\sqrt{\pi\nu\hat{\sigma}^2}} \left(1 + \frac{1}{\nu} \frac{(\mu - \mu_N)^2}{\hat{\sigma}^2}\right)^{-\frac{\nu+1}{2}} \\
&= T_\nu(\mu; \mu_N, \hat{\sigma}^2),
\end{aligned}$$

with:

- $\nu = 2\alpha_N$,
- $\hat{\sigma}^2 = \frac{\beta_N}{\alpha_N \lambda_N}$.

The marginal posterior distribution over μ can thus be expressed as a non-standardised Student's t -distribution that we express below in terms of the initial hyper-parameters:

$$\mu | \mathbf{y} \sim T_{2\alpha_0 + N} \left(\frac{N\bar{y} + \lambda_0\mu_0}{\lambda_0 + N}, \frac{\beta_0 + \frac{1}{2} \sum_{n=1}^N (y_n - \bar{y})^2 + \frac{\lambda_0 N}{2(\lambda_0 + N)} (\bar{y} - \mu_0)^2}{(\alpha_0 + \frac{N}{2})(\lambda_0 + N)} \right). \quad (2)$$

The derivation of this analytical formula provides a valuable tool for computing straightforward posterior distribution for the mean parameter in such a context. We shall see in the next section how to leverage this approach to introduce a novel means' comparison methodology for a more general framework to handle both multidimensional and missing data.

2.2 General Bayesian framework for evaluating mean differences

Recalling our differential proteomics context that assesses the differences in mean intensity values for P peptides or proteins quantified in N samples divided into K conditions. As before, Figure 2 illustrates the hierarchical generative structure assumed for each group $k = 1, \dots, K$.

Maintaining the notation analogous to previous ones, the generative model for $\mathbf{y}_k \in \mathbb{R}^P$, can be written as:

$$\mathbf{y}_k = \boldsymbol{\mu}_k + \boldsymbol{\varepsilon}_k, \quad \forall k = 1, \dots, K,$$

where:

- $\boldsymbol{\mu}_k | \boldsymbol{\Sigma}_k \sim \mathcal{N}\left(\boldsymbol{\mu}_0, \frac{1}{\lambda_0} \boldsymbol{\Sigma}_k\right)$ is the prior mean intensities vector of the k -th group,
- $\boldsymbol{\varepsilon}_k \sim \mathcal{N}(0, \boldsymbol{\Sigma}_k)$ is the error term of the k -th group,
- $\boldsymbol{\Sigma}_k \sim \mathcal{W}^{-1}(\boldsymbol{\Sigma}_0, \nu_0)$ is the prior variance-covariance matrix of the k -th group,

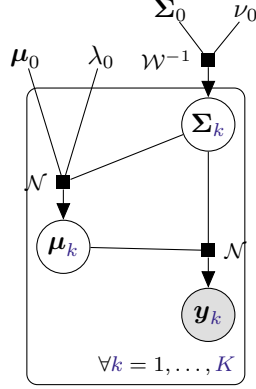


Figure 2: Graphical model of the hierarchical structure of the generative model for the vector \mathbf{y}_k of peptide intensities in K groups of biological samples, *i.e.* K experimental conditions.

with $\{\boldsymbol{\mu}_0, \lambda_0, \boldsymbol{\Sigma}_0, \nu_0\}$ a set of hyper-parameters that needs to be chosen as modelling hypotheses and \mathcal{W}^{-1} represents the inverse-Wishart distribution, used as the conjugate prior for an unknown covariance matrix of a multivariate Gaussian distribution (Bishop, 2006).

Traditionally, in Bayesian inference, those quantities must be carefully chosen for the estimation to be as accurate as possible, particularly with low sample sizes. Incorporating expert or prior knowledge in the model would also come from the adequate setting of these hyper-parameters. However, our final purpose in this article is not much about estimating but comparing groups' mean (*i.e.* differential analysis). Interestingly, providing a perfect estimation of the posterior distributions over $\{\boldsymbol{\mu}_k\}_{k=1,\dots,K}$ does not appear as the main concern here, as the posterior difference of means (*i.e.* $p(\boldsymbol{\mu}_k - \boldsymbol{\mu}_{k'} \mid \mathbf{y}_k, \mathbf{y}_{k'})$) represents the actual quantity of interest. Although providing meaningful prior hyper-parameters leads to adequate uncertainty quantification, we shall, above all, take those quantities equal for all groups. This choice would ensure an unbiased comparison, constituting a valuable alternative to the traditional and somehow limited t -tests. Indeed, inference based on hypothesis testing and p-values has been widely questioned over the past decade (Wasserstein et al., 2019). Additionally, t -tests do not provide insight into effect sizes or uncertainty quantification (in contrast to Bayesian inference as emphasised by Kruschke and Liddell (2018)).

The present framework aspires to estimate a posterior distribution for each mean parameter vector $\boldsymbol{\mu}_k$, starting from the same prior assumptions in each group. The comparison between the means of all groups would then only rely on the ability to sample directly from these distributions and compute empirical posteriors for the means' difference. As a bonus, this framework remains compatible with multiple imputations strategies previously introduced to handle missing data that frequently arise in applicative contexts (Chion et al., 2022).

From the previous hypotheses, we can deduce the likelihood of the model for an i.i.d. sample $\{\mathbf{y}_{k,1}, \dots, \mathbf{y}_{k,N_k}\}$:

$$\begin{aligned} p(\mathbf{y}_{k,1}, \dots, \mathbf{y}_{k,N_k} \mid \boldsymbol{\mu}_k, \boldsymbol{\Sigma}_k) &= \prod_{n=1}^{N_k} p(\mathbf{y}_{k,n} \mid \boldsymbol{\mu}_k, \boldsymbol{\Sigma}_k) \\ &= \prod_{n=1}^{N_k} \mathcal{N}(\mathbf{y}_{k,n}; \boldsymbol{\mu}_k, \boldsymbol{\Sigma}_k), \end{aligned}$$

However, as previously pointed out, such datasets often contain missing data, and we shall introduce here consistent notation. Assume \mathcal{H} to be the set of all observed data, we additionally define:

- $\mathbf{y}_k^{(0)} = \{\mathbf{y}_{k,n}^p \in \mathcal{H}, n = 1, \dots, N_k, p = 1, \dots, P\}$, the set of elements that are observed in the k -th group,
- $\mathbf{y}_k^{(1)} = \{\mathbf{y}_{k,n}^p \notin \mathcal{H}, n = 1, \dots, N_k, p = 1, \dots, P\}$, the set of elements that are missing the k -th group.

Moreover, as we remain in the context of multiple imputation, we define $\{\tilde{\mathbf{y}}_k^{(1),1}, \dots, \tilde{\mathbf{y}}_k^{(1),D}\}$ as the set of D draws of an imputation process applied on missing data in the k -th group. In such context, a closed-form approximation for the multiple-imputed posterior distribution of $\boldsymbol{\mu}_k$ can be derived for each group as stated in Proposition 1.

Proposition 1. *For all $k = 1, \dots, K$, the posterior distribution of $\boldsymbol{\mu}_k$ can be approximated by a mixture of multiple-imputed multivariate t -distributions, such as:*

$$p(\boldsymbol{\mu}_k | \mathbf{y}_k^{(0)}) \simeq \frac{1}{D} \sum_{d=1}^D T_{\nu_k} \left(\boldsymbol{\mu}; \tilde{\boldsymbol{\mu}}_k^{(d)}, \tilde{\boldsymbol{\Sigma}}_k^{(d)} \right)$$

with:

- $\nu_k = \nu_0 + N_k - P + 1$,
- $\tilde{\boldsymbol{\mu}}_k^{(d)} = \frac{\lambda_0 \boldsymbol{\mu}_0 + N_k \tilde{\mathbf{y}}_k^{(d)}}{\lambda_0 + N_k}$,
- $\tilde{\boldsymbol{\Sigma}}_k^{(d)} = \frac{\boldsymbol{\Sigma}_0 + \sum_{n=1}^{N_k} (\tilde{\mathbf{y}}_{k,n}^{(d)} - \bar{\mathbf{y}}_k^{(d)})(\tilde{\mathbf{y}}_{k,n}^{(d)} - \bar{\mathbf{y}}_k^{(d)})^\top + \frac{\lambda_0 N_k}{(\lambda_0 + N_k)} (\bar{\mathbf{y}}_k^{(d)} - \boldsymbol{\mu}_0)(\bar{\mathbf{y}}_k^{(d)} - \boldsymbol{\mu}_0)^\top}{(\nu_0 + N_k - P + 1)(\lambda_0 + N_k)}$,

where we introduced the shorthand $\tilde{\mathbf{y}}_{k,n}^{(d)} = \begin{bmatrix} \mathbf{y}_{k,n}^{(0)} \\ \tilde{\mathbf{y}}_{k,n}^{(1),d} \end{bmatrix}$ to represent the d -th imputed vector of observed data, and the corresponding average vector $\bar{\mathbf{y}}_k^{(d)} = \frac{1}{N_k} \sum_{n=1}^{N_k} \tilde{\mathbf{y}}_{k,n}^{(d)}$.

This analytical formulation is particularly convenient for our purpose and, as we shall see in the proof in section 7.2, merely comes from imputation.

Thanks to Proposition 1, we have an explicit formula for approximating, using multiple-imputed datasets, the posterior distribution of the mean vector for each group. Although such a linear combination of multivariate t -distributions is not a known specific distribution in itself, it is now straightforward to generate realisations of samples of the posterior by simply drawing from the D multivariate t -distributions, each being specific to an imputed dataset, and then compute the mean of the D vectors. Therefore, the empirical distribution resulting from a high number of samples generated by this procedure would be easy to visualise and manage for comparison purposes. Generating the empirical distribution of the mean's difference between two groups k and k' then comes directly by computing the difference between each couple of samples drawn from both posterior distributions $p(\boldsymbol{\mu}_k | \mathbf{y}_k^{(0)})$ and $p(\boldsymbol{\mu}_{k'} | \mathbf{y}_{k'}^{(0)})$. In Bayesian statistics, relying on empirical distributions drawn from the posterior is common practice in the context of Markov chain Monte Carlo (MCMC) algorithms but often comes at a high computational cost. In our framework, we managed to maintain the best of both worlds since deriving analytical distributions from model hypotheses offers the benefits of probabilistic inference with adequate uncertainty quantification while remaining tractable and not relying on MCMC procedures. The computational cost of the method thus roughly remains as low as frequentist counterparts since merely a few updating calculus and drawing from t -distributions are needed. Empirical evidence of this claim is provided in the dedicated simulation study proposed further in Table 3.

As usual, when it comes to comparing the mean between two groups, we still need to assess if the posterior distribution of the difference appears, in a sense, to be sufficiently away from zero. This practical inference choice is not specific to our context and remains highly dependent on the context of the study. Moreover, as the present model is multi-dimensional, we may also question the metric used to compute the difference between vectors. In a sense, our posterior distribution of the mean's differences offers an elegant solution to the traditional problem of multiple testing often encountered in applied science and allows tailored definitions of what could be called a *meaningful* result (*significant* does not appear anymore as an appropriate term in this more general context). For example, displaying the distribution of the squared difference would penalise large differences in elements of the mean vector. In contrast, the absolute difference would give a more balanced

conception of the average divergence from one group to the other. Clearly, as any marginal of a multivariate t -distribution remains a (multivariate) t -distribution, comparing specific elements of the mean vectors merely by restraining to the appropriate dimension is also straightforward. In particular, comparing two groups in the univariate case would be a particular case of Proposition 1 with $P = 1$. Recalling our proteomics context, we could still compare the mean intensity of peptides between groups, one peptide at a time, or choose to compare all peptides at once and thus accounting for possible correlations between peptides in each group. However, an appropriate manner of accounting for those correlations could be to subset peptides using their protein groups.

Let us provide in Algorithm 1 a summary of the procedure for comparing mean vectors of two different experimental conditions regarding posterior distribution.

Algorithm 1 Posterior distribution of the vector of mean's difference

Initialise the hyper-posteriors $\boldsymbol{\mu}_0^k = \boldsymbol{\mu}_0^{k'}$, $\lambda_0^k = \lambda_0^{k'}$, $\boldsymbol{\Sigma}_0^k = \boldsymbol{\Sigma}_0^{k'}$, $\nu_0^k = \nu_0^{k'}$

for $d = 1, \dots, D$ **do**

 Compute $\{\boldsymbol{\mu}_N^{k,(d)}, \lambda_N^k, \boldsymbol{\Sigma}_N^{k,(d)}, \nu_N^k\}$ and $\{\boldsymbol{\mu}_N^{k',(d)}, \lambda_N^{k'}, \boldsymbol{\Sigma}_N^{k',(d)}, \nu_N^{k'}\}$ from hyper-posteriors and data

 Draw R realisations $\hat{\boldsymbol{\mu}}_k^{(d)[r]} \sim T_{\nu_N^k} \left(\boldsymbol{\mu}_N^{k,(d)}, \frac{\boldsymbol{\Sigma}_N^{k,(d)}}{\lambda_N^k \nu_N^k} \right)$; $\hat{\boldsymbol{\mu}}_{k'}^{(d)[r]} \sim T_{\nu_N^{k'}} \left(\boldsymbol{\mu}_N^{k',(d)}, \frac{\boldsymbol{\Sigma}_N^{k',(d)}}{\lambda_N^{k'} \nu_N^{k'}} \right)$

end for

for $r = 1, \dots, R$ **do**

 Compute $\hat{\boldsymbol{\mu}}_k^{[r]} = \frac{1}{D} \sum_{d=1}^D \hat{\boldsymbol{\mu}}_k^{(d)[r]}$ and $\hat{\boldsymbol{\mu}}_{k'}^{[r]} = \frac{1}{D} \sum_{d=1}^D \hat{\boldsymbol{\mu}}_{k'}^{(d)[r]}$ to combine samples

 Generate a realisation $\hat{\boldsymbol{\mu}}_\Delta^{[r]} = \hat{\boldsymbol{\mu}}_k^{[r]} - \hat{\boldsymbol{\mu}}_{k'}^{[r]}$ from the difference's distribution

end for

return $\{\hat{\boldsymbol{\mu}}_\Delta^{[1]}, \dots, \hat{\boldsymbol{\mu}}_\Delta^{[R]}\}$, an R -sample drawn from the posterior distribution of the mean's difference

2.3 The uncorrelated case: no more multiple testing nor imputation

Let us notice that modelling covariances between all variables as in Proposition 1 often constitutes a challenge, which is computationally expensive in high dimensions and not always adapted. However, we detailed in Section 2.1 results that are classical in Bayesian inference but not widespread enough in applied science, especially when comparing means. In particular, we can leverage these results to adapt Algorithm 1 to the univariate case for handling the same problem as in Chion et al. (2022) with a more probabilistic flavour. Indeed, when the absence of correlations between peptides is assumed (*i.e.* $\boldsymbol{\Sigma}$ being diagonal), the problem reduces to the analysis of P independent inference problems (as $\boldsymbol{\mu}$ is supposed Gaussian) and the posterior distributions can be derived in closed-form, as we recalled in Equation (1). Moreover, let us highlight a nice property coming with this relaxing assumption is that (multiple-)imputation is no longer needed in this context. Using the same notation as before and the uncorrelated assumption (and thus the induced independence between analytes for $p \neq p'$), we can write:

$$p(\boldsymbol{\mu}_k | \mathbf{y}_k^{(0)}) = \int p(\boldsymbol{\mu}_k, \mathbf{y}_k^{(1)} | \mathbf{y}_k^{(0)}) d\mathbf{y}_k^{(1)} \quad (3)$$

$$= \int p(\boldsymbol{\mu}_k | \mathbf{y}_k^{(0)}, \mathbf{y}_k^{(1)}) p(\mathbf{y}_k^{(1)} | \mathbf{y}_k^{(0)}) d\mathbf{y}_k^{(1)} \quad (4)$$

$$= \int \prod_{p=1}^P \left\{ p(\mu_k^p | y_k^{p,(0)}, y_k^{p,(1)}) p(y_k^{p,(1)} | y_k^{p,(0)}) \right\} d\mathbf{y}_k^{(1)} \quad (5)$$

$$= \prod_{p=1}^P \int \left\{ p\left(\mu_k^p \mid y_k^{p,(0)}, y_k^{p,(1)}\right) p\left(y_k^{p,(1)} \mid y_k^{p,(0)}\right) dy_k^{p,(1)} \right\} \quad (6)$$

$$= \prod_{p=1}^P p\left(\mu_k^p \mid y_k^{p,(0)}\right) \quad (7)$$

$$= \prod_{p=1}^P T_{2\alpha_0^p + N_k^p} \left(\mu_k^p; \mu_{k,N}^p, \hat{\sigma}_k^{p2} \right), \quad (8)$$

with:

$$\begin{aligned} \bullet \mu_{k,N}^p &= \frac{N_k^p \bar{y}_k^{p,(0)} + \lambda_0^p \mu_0^p}{\lambda_0^p + N_k^p}, \\ \bullet \hat{\sigma}_k^{p2} &= \frac{\beta_0^p + \frac{1}{2} \sum_{n=1}^{N_k^p} (y_{k,n}^{p,(0)} - \bar{y}_k^{p,(0)})^2 + \frac{\lambda_0^p N_k^p}{2(\lambda_0^p + N_k^p)} (\bar{y}_k^{p,(0)} - \mu_0^p)^2}{(\alpha_0^p + \frac{N_k^p}{2})(\lambda_0^p + N_k^p)}. \end{aligned}$$

In this context, it can be noticed that $p\left(\boldsymbol{\mu}_k \mid \mathbf{y}_k^{(0)}\right)$ factorises naturally over $p = 1, \dots, P$, and thus only depends upon the data that have actually been observed for each peptide. Indeed, we observe that the integration over the missing data $\mathbf{y}_k^{(1)}$ is straightforward in this framework, and neither Rubin’s approximation nor even imputation (whether multiple or not) appears necessary. The observed data $\mathbf{y}_k^{(0)}$ already bear all the useful information as if each unobserved value could simply be ignored without effect on the posterior distribution.

Let us emphasise that this property of factorisation and tractable integration over missing data comes directly from the covariance structure as a diagonal matrix and thus only constitutes a particular case of the previous model, though convenient. However, in the context of differential analysis in proteomics, analysing each peptide as an independent problem is a common practice, as seen in [Chion et al. \(2022\)](#), and we shall notice that the Bayesian framework tackles this issue in an elegant and somehow simpler way. In particular, the classical inference approach based on hypothesis testing performs numerous successive tests for all peptides. Such an approach often leads to the pitfall of multiple testing that must be carefully dealt with. Interestingly, we notice that the above model also avoids multiple testing (as it does not rely on hypothesis testing and the definition of some threshold) while maintaining the convenient interpretations of Bayesian probabilistic inference. To conclude, whereas the analytical derivation of posterior distributions with Gaussian-inverse-gamma constitutes a well-known result, our proposition to define such probabilistic mean’s comparison procedure provides, under the standard uncorrelated-peptides assumption, an elegant and handy alternative to classical techniques that naturally tackles both the imputation and multiple testing issues.

Let us provide in [Algorithm 2](#) the pseudo-code of the inference procedure to highlight differences with the fully-correlated case:

3 Experiments

3.1 Simulated datasets

To generate simulated datasets to evaluate the performances of our method, called ProteoBayes, we used the generative model presented in [Figure 1](#). A Gaussian distribution $\mathcal{N}(0, 1)$ is taken as a baseline reference. To compute mean differences between groups, we will generate samples from various distribution $\mathcal{N}(m, \sigma^2)$ where m and σ^2 will vary depending on the context. Unless otherwise stated, each experiment is repeated 1000 times, and results are averaged to computed mean values and standard deviation of the metrics. In each group, we observe 5 distinct samples. The quality of estimation is evaluated in terms of Root Mean Squared Error (RMSE) and 95% Credible Interval Coverage (CIC_{95}). The mean differences between groups and the width of the 95% Credible Interval will also be reported to assess the performance of the method. Results are compared with a standard

Algorithm 2 Posterior distribution of the mean’s difference

for $p = 1, \dots, P$ **do**

 Initialise the hyper-posteriors $\mu_0^{k,p} = \mu_0^{k',p}$, $\lambda_0^{k,p} = \lambda_0^{k',p}$, $\alpha_0^{k,p} = \alpha_0^{k',p}$, $\beta_0^{k,p} = \beta_0^{k',p}$

 Compute $\{\mu_N^{k,p}, \lambda_N^{k,p}, \alpha_N^{k,p}, \beta_N^{k,p}\}$ and $\{\mu_N^{k',p}, \lambda_N^{k',p}, \alpha_N^{k',p}, \beta_N^{k',p}\}$ from hyper-posteriors and data

 Draw R realisations $\hat{\mu}_k^{p,[r]} \sim T_{\alpha_N^{k,p}} \left(\mu_N^{k,p}, \frac{\beta_N^{k,p}}{\lambda_N^{k,p} \alpha_N^{k,p}} \right)$, $\hat{\mu}_{k'}^{p,[r]} \sim T_{\alpha_N^{k',p}} \left(\mu_N^{k',p}, \frac{\beta_N^{k',p}}{\lambda_N^{k',p} \alpha_N^{k',p}} \right)$

for $r = 1, \dots, R$ **do**

 Generate a realisation $\hat{\mu}_\Delta^{p,[r]} = \hat{\mu}_k^{p,[r]} - \hat{\mu}_{k'}^{p,[r]}$ from the difference’s distribution

end for

end for

return $\{\hat{\mu}_\Delta^{[1]}, \dots, \hat{\mu}_\Delta^{[R]}\}$, an R -sample drawn from the posterior distribution of the mean’s difference

t-test, for which the associated p-value is reported. Throughout the experiment section, we used the following values for prior parameters:

- $\mu_0 = \bar{y}$,
- $\lambda = 1$,
- $\alpha_0 = 1$,
- $\beta_0 = 1$,
- $\Sigma_0 = I_P$,
- $\nu_0 = 10$,

where \bar{y} represent the average of observed values computed over all groups. These values correspond to the practical insights acquired from our previous studies while remaining relatively vague in terms of prior variance. As previously stated, it is essential for these values to be identical in all groups to ensure a fair and unbiased comparison. In the case where more expert information would be accessible, its incorporation would be possible, for instance, through the definition of a more precise prior mean (μ_0) associated with a more confident prior variance (encoded through α_0 and β_0).

3.2 Real datasets

To illustrate our methodology, we used a real proteomics dataset already introduced in [Chion et al. \(2022\)](#), namely the *Arabidopsis thaliana* + UPS dataset, with the Match between Runs algorithm and at least one quantified value in each experimental condition. Briefly, let us recall that UPS proteins were spiked in increasing amounts into a constant background of *Arabidopsis thaliana* (ARATH) protein lysate. Hence, UPS proteins are differentially expressed, and ARATH proteins are not. For illustration purposes, we arbitrarily focused the examples on the P12081ups|SYHC_HUMAN_UPS and the sp|F4I893|ILA_ARATH proteins. Note that both proteins have nine quantified peptides. Unless otherwise stated, we took the examples of the AALEELVK UPS peptide and the VLPLIIPILSK ARATH peptide and the same values as for synthetic data have been set for the prior hyper-parameters.

Additionally, let us recall that in our real datasets, the constants have the following values:

- $\forall k = 1, \dots, K$, $N_k = 3$ data points, in the absence of missing data,
- $P = 9$ peptides, when using the multivariate model,
- $D = 7$ draws of imputation,
- $R = 10^4$ sample points from the posterior distributions.

	ProteoBayes		t-test	Quality of estimation	
	Mean difference	CI ₉₅ width	p_value	RMSE	CIC ₉₅
$\mathcal{N}(1, 1)$	1 (0.04)	0.12 (0.003)	10^{-79} (10^{-78})	0.03 (0.04)	95.7 (20.3)
$\mathcal{N}(5, 1)$	4.99 (0.04)	0.12 (0.003)	0 (0)	0.03 (0.04)	94.6 (22.61)
$\mathcal{N}(10, 1)$	9.99 (0.04)	0.13 (0.003)	0 (0)	0.03 (0.04)	95.9 (19.84)
$\mathcal{N}(1, 5)$	1 (0.16)	0.6 (0.01)	10^{-06} (10^{-6})	0.16 (0.19)	95.5 (20.74)
$\mathcal{N}(1, 10)$	0.99 (0.31)	1.2 (0.02)	0.03 (0.08)	0.31 (0.37)	95 (21.81)
$\mathcal{N}(1, 20)$	1.04 (0.58)	2.4 (0.06)	0.22 (0.26)	0.62 (0.75)	95.2 (21.39)

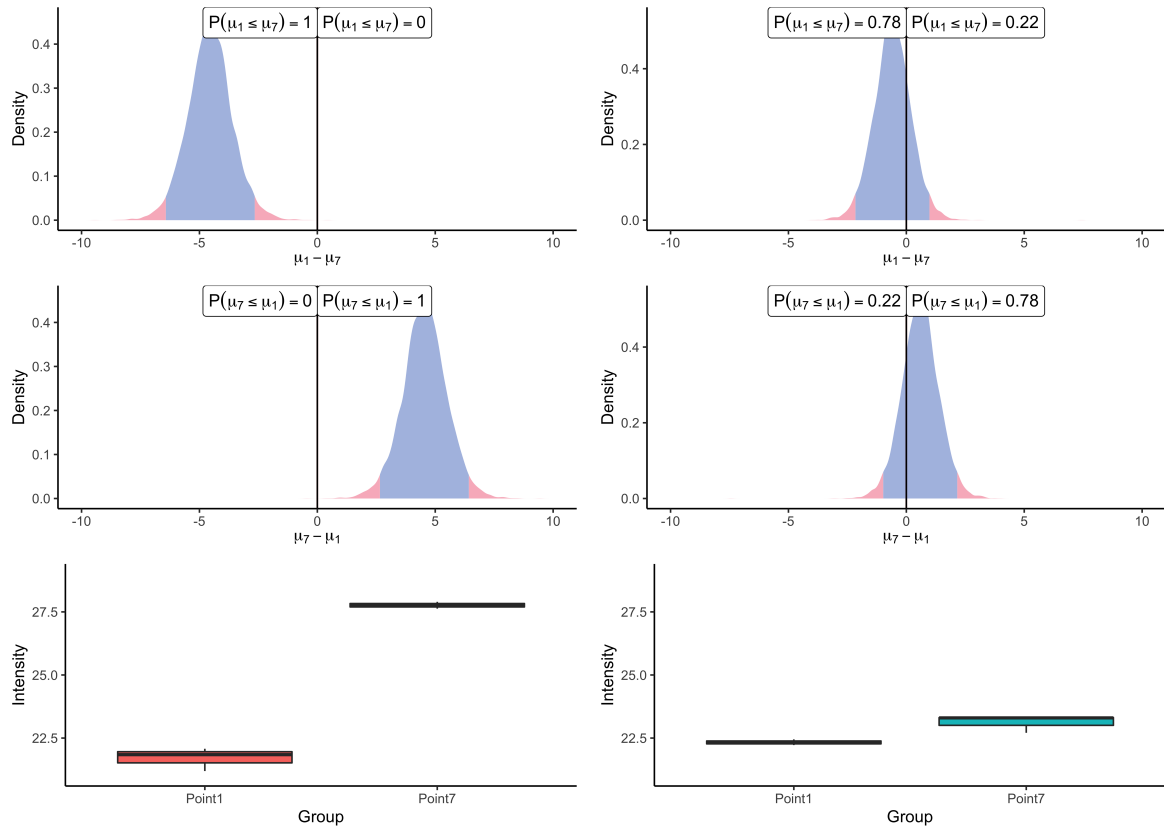
Table 2: Simulation study reporting performances of univariate ProteoBayes compared to a standard t-test. All distributions are compared with the univariate Gaussian baseline $\mathcal{N}(0, 1)$. All results are averaged over 1000 repetitions of the experiments and reported using the format *Mean (Sd)*.

In this context, where the number N_k of observed biological samples is extremely low, particularly when data are missing, we should expect a perceptible influence of the prior hyper-parameters and a perceptible influence of inherent uncertainty in the posteriors. However, this influence has been reduced to the minimum in all the subsequent graphs for the sake of clarity and to ensure a good understanding of the underlying properties of the methodology. The high number R of sample points drawn from the posteriors assures the empirical distribution to be smoothly displayed on the graph. Still, one should note that sampling is really quick in practice, and this number can be easily increased if necessary.

3.3 Univariate Bayesian inference for differential analysis

First, let us illustrate the univariate framework described in Section 2.3. In this experiment, we compared the intensity means in the lowest (0.05 fmol UPS) and the highest points (10 fmol UPS) of the UPS spike range. Let us recall that our univariate algorithm does not rely on imputation and should be applied directly to raw data. For the sake of illustration, the chosen peptides were observed entirely in all three biological samples of both experimental conditions. Resulting of the application of our univariate algorithm, posterior distributions of the mean difference for both peptides are represented on Figure 3. As the analysis consists of a comparison between conditions, the 0 value has been highlighted on the x-axis for assessing both the direction and the magnitude of the difference. The distance to zero of the distributions indicates whether the peptide is differentially expressed or not. In particular, Figure 3a shows the posterior distribution of the means' difference for the UPS peptide. Its location, far from zero, indicates a high probability (almost surely in this case) that the mean intensity of this peptide differs between the two considered groups. Conversely, the posterior distribution of the difference of means for the ARATH peptide (Figure 3b) suggests that the probability that means differ is low. Those conclusions support the summaries of raw data depicted on the bottom panel of Figure 3. Moreover, the posterior distribution provides additional insights into whether a peptide is under-expressed or over-expressed in a condition compared to another. For example, looking back to the UPS peptide, Figure 3a suggests an over-expression of the AALEELVK peptide in the seventh group (being the condition with the highest amount of UPS spike) compared to the first group (being the condition with the lowest amount of UPS spike), which is consistent with the experimental design. Furthermore, the middle panel merely highlights the fact that the posterior distribution of the difference $\mu_1 - \mu_7$ is symmetric of $\mu_7 - \mu_1$, thus, the sense of the comparison only remains an aesthetic choice.

To pursue further the illustration and evaluation of ProteoBayes at a larger scale, we provided in Table 2 a thorough analysis of mean differences computation for various effect size and variance combinations. One can notice that, in all cases, we recover values that are, on average, remarkably close to the true mean difference. As expected, increasing the variance in the data would result in larger credible intervals as the computed posterior distributions adapt to the higher uncertainty context. Even though this issue is often pointed out in the literature, p-values coming from the t-test in these experiments seem particularly uninformative in this context. Their values are so close to 0 that it is generally difficult to assess how much the two groups are close, with an adequate degree of caution. Moreover, these results were all computed for a sample size equal to 5, though it is



(a) AALEELVK peptide from the P12081ups|SYHC_HUMAN_UPS protein. (b) VLPLIIPILSK peptide from the sp|F4I893|ILA_ARATH protein.

Figure 3: **Posterior distributions of the difference of means between the 0.05 fmol UPS spike condition (μ_1) and the 10 fmol UPS spike condition (μ_7) and the corresponding boxplots summarising the observed data.** The 95% credible interval is indicated by the blue central region.

well known that p-values can change dramatically depending on sample size, regardless of the true underlying difference between groups. A drawback that is often associated with Bayesian methods lies in the increasing computational burden compared to frequentist counterparts. However, by leveraging conjugate priors in our model and relying on sampling from analytical distributions to conduct inference, we managed to maintain a (univariate) algorithm as quick as t-tests in practice, as illustrated in Table 3. As expected, the multivariate version is generally slightly longer to run as we need to estimate covariance matrices that typically grow quickly with the number of peptides simultaneously modelled. That said, let us point out that we can still easily scale up to many thousands of peptides in a reasonable time (from a few seconds to minutes).

	Univariate	Multivariate	T-test
$P = 10^2$	0.08	0.8	0.22
$P = 10^3$	1.75	4.91	1.33
$P = 10^4$	6.80	58.96	6.38

Table 3: Running times (in seconds) of univariate and multivariate ProteoBayes compared with standard t-test for increasing numbers of peptides.

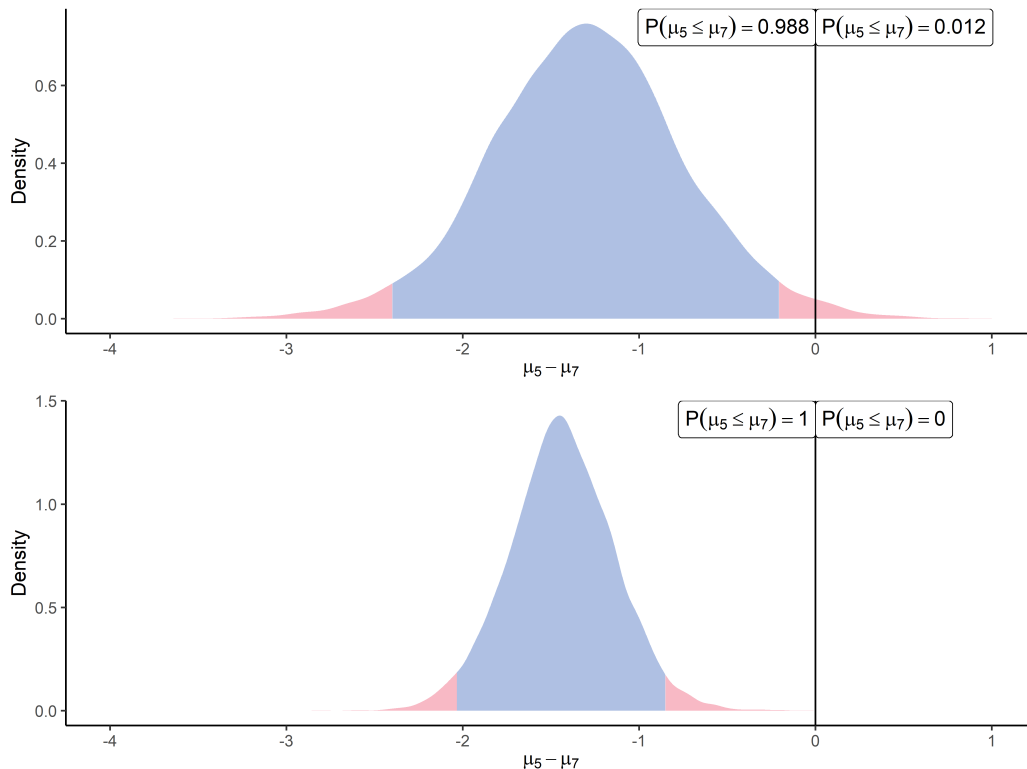


Figure 4: Posterior distributions of the mean difference $\mu_5 - \mu_7$ for the AALEELVK peptide from the P12081ups|SYHC_HUMAN_UPS protein using the univariate approach (top) and the multivariate approach (bottom). The blue central region indicates the 95% credible interval.

		Mean difference	CI_{95} width
Univariate	$\mathcal{N}_{10}(\mathbf{0}_{10}, 0.9 \times \mathbf{I}_{10} + \mathbf{0.1}_{10 \times 10})$	0.92 (0.02)	1.29 (0.03)
	$\mathcal{N}_{10}(\mathbf{0}_{10}, \mathbf{0.1}_{10 \times 10})$	0.9 (0.03)	1.69 (0.04)
Multivariate	$\mathcal{N}_{10}(\mathbf{0}_{10}, 0.9 \times \mathbf{I}_{10} + \mathbf{0.1}_{10 \times 10})$	0.93 (0.02)	0.93 (0.04)
	$\mathcal{N}_{10}(\mathbf{0}_{10}, \mathbf{1}_{10 \times 10})$	0.89 (0.03)	1.28 (0.06)

Table 4: Comparison of univariate and multivariate versions of ProteoBayes in terms of computed mean differences and associated uncertainty. This baseline comparison is the multivariate Gaussian $\mathcal{N}_{10}(\mathbf{0}_{10}, I_{10})$.

3.4 The benefit of intra-protein correlation

One of the main benefits of our methodology is to account for between-peptides correlation, as described in Section 2.2. As the first illustration of such a property, we modelled correlations between all quantified peptides derived from the same protein. In order to highlight the gains that we may expect from such modelling, we displayed on Figure 4 the comparison between a differential analysis using our univariate method or using the multivariate approach. In this example, we purposefully considered a group of 9 peptides coming from the same protein (P12081ups|SYHC_HUMAN_UPS), which intensities may undoubtedly be correlated to some degree. We consider in this section the comparison of intensity means between the fifth point (2.5 fmol UPS - μ_5) and the seventh point (10 fmol UPS - μ_7) of the UPS spike range. The posterior difference of the mean vector $\mu_5 - \mu_7$ between two conditions has been computed, and the first peptide (AALEELVK) has been extracted for graphical visualisation. Meanwhile, the univariate algorithm has also been applied to compute the posterior difference $\mu_5 - \mu_7$, solely on the peptide AALEELVK. The top panel of Figure 4 displays the latter approach, while the multivariate case is exhibited on the bottom panel. One should observe clearly that, while the location parameter of the two distributions is close as expected, the multivariate

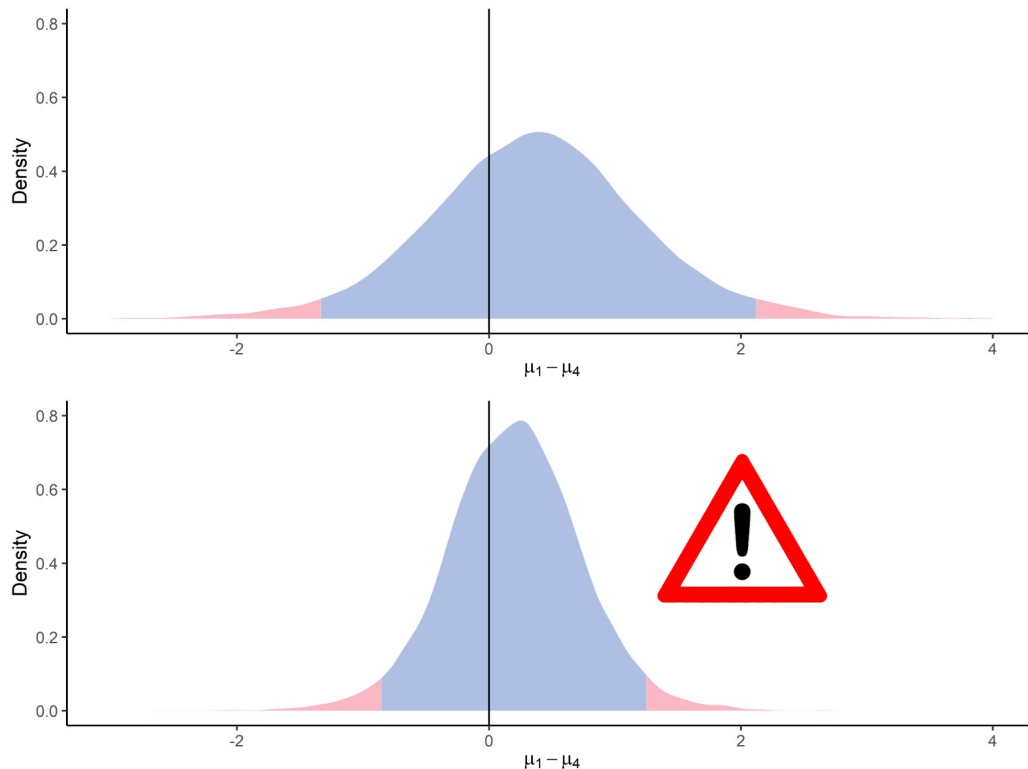


Figure 5: Posterior distributions of the mean difference $\mu_1 - \mu_4$ for the EVQELAQEEAER peptide from the sp|F4I893|ILA_ARATH protein using the observed dataset (top) and the imputed dataset (bottom)

approach takes advantage of the information coming from the correlated peptides to reduce the uncertainty in the posterior estimation. To confirm this visual intuition, we provided in Table 4 additional evidence from synthetic datasets highlighting the tighter credible intervals obtained thanks to the multivariate modelling and accounting for inter-peptide correlations. This tighter range of probable values leads to a more precise estimation of the effect size and increased confidence in the resulting inference (deciding whether the peptide is differential or not).

3.5 The mirage of imputed data

After discussing the advantages and the valuable interpretative properties of our methods, let us mention a pitfall that one should avoid for the inferences to remain valid. In the case of univariate analysis, we pointed out with Equation (3) that all the useful information is contained in observed data, and no imputation is needed since we already integrated out all missing data. Imputation does actually not even make sense in one dimension since, by definition, a missing data point is simply equivalent to an unobserved one, and we shall gain more information only by collecting more data. Therefore, one should be really careful when dealing with imputed datasets and keep in mind that imputation somehow *creates* new data points that do not bear any additional information. Thus, there is a risk of artificially decreasing the uncertainty of our estimated posterior distributions simply by considering more data points in the computations than what was genuinely observed. For instance, imagine a dummy example where 10 points are effectively observed, and 1000 remain missing. It would be a massive error and underestimation of the true variance to impute the 1000 missing points (say with the average of the ten observed ones) and use the resulting 1010-dimensional vector for computing the posterior distributions of the mean. Let us mention that such a problem is not specific to our framework and, more generally, also applies to Rubin's rules. One should keep in mind that those approximations only hold for a reasonable ratio of missing data. Otherwise, one may consider adapting the method, for example, by penalising the degree of freedom in the relevant t -distributions. To illustrate this issue, we displayed on Figure 5 an example of our univariate algorithm

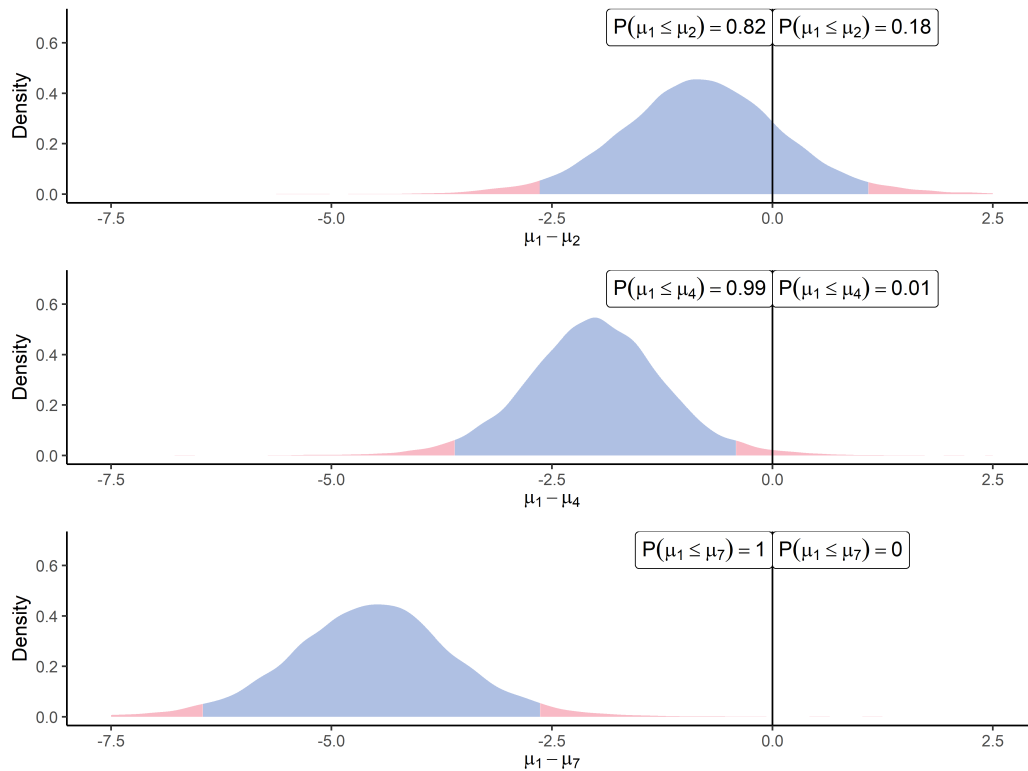


Figure 6: Posterior distributions of the mean differences $\mu_1 - \mu_2$, $\mu_1 - \mu_4$ and $\mu_1 - \mu_7$ for the AALEELVK peptide from the P12081ups|SYHC_HUMAN_UPS protein.

applied both on the observed dataset (top panel) and the imputed dataset (bottom panel). In this context, we observe a reduced variance for the imputed data. However, this behaviour is just an artefact of the phenomenon mentioned above: the bottom graph is merely not valid, and only raw data should be used in our univariate algorithm to avoid spurious inference results. More generally, while imputation is sometimes needed for the methods to work, one should always keep in mind that it always constitutes a bias (although controlled) that should be accounted for with tailored solutions, as this manuscript intends to provide.

3.6 Acknowledging the effect size

After discussing methodological aspects, let us dive into more biological-related properties displayed on Figure 6. The three panels describe the increasing differences that can be observed when we sequentially compare the first point (0.05 fmol UPS) of the UPS spike range (μ_1) to the second one (0.25 fmol UPS - μ_2), the fourth one (1.25 fmol UPS - μ_4) and the highest one (25 fmol UPS - μ_7). The experimental design suggests that the difference in means for a UPS peptide should increase with respect to the amount of UPS proteins that was spiked in the biological sample (Chion et al., 2022). This illustration offers a perspective on how this difference becomes more and more noticeable, though mitigated by the inherent variability. Such an explicit and adequately quantified variance, and the induced uncertainty in the estimation, should help practitioners to make more educated decisions with the appropriate degree of caution. In particular, Figure 6 highlights the importance of considering the effect size (increasing here), which is crucial when studying the underlying biological phenomenon. Such a graph may remind us that statistical inference should be more about offering helpful insights to experts of a particular domain rather than defining automatic and blind decision-making procedures (Betensky, 2019). Moreover, let us point out that current statistical tests used for differential analysis express their results solely as p -values. One should keep in mind that, no matter their value, they do not provide any information about the effect size of the phenomenon (Sullivan and Feinn, 2012).

3.7 About protein inference

To conclude on the practical usage of the proposed multivariate algorithm, let us develop ideas for comparing simultaneously multiple peptides or proteins. As highlighted before, accounting for the covariances between peptides tends to reduce the uncertainty on the posterior distribution of a unique peptide. However, we only exhibited examples comparing one peptide at a time between two conditions, although in applications, practitioners often need to compare thousands of them simultaneously. From a practical point of view, while possible in theory, we probably want to avoid modelling the correlations between every combination of peptides into a full rank matrix for at least two reasons.

First, it probably does not bear much sense to assume that all peptides in a biological sample interact with no particular structure. Secondly, it appears unreasonable to do so from a statistical and practical point of view. Computing and storing a matrix with roughly 10^4 rows and columns induces a computational and memory burden that would complicate the procedure while potentially leading to unreliable objects if matrices are estimated merely on a few data points, as for our example. However, a more promising approach would consist in deriving a sparse approach by leveraging the underlying structure of data from a biological perspective. If we reasonably assume, as before, that only peptides from common proteins present non-negligible correlations, it is then straightforward to define a block-diagonal matrix for the complete vector of peptides, which would be far more reasonable to estimate. Such an approach would take advantage of both of our algorithms by using the factorisation (as in Equation (3)) over thousands of proteins to sequentially estimate a high number of low dimensional mean vectors. Assuming an example with a thousand proteins containing ten peptides each, the approximate computing and storage requirements would be reduced from a $(10^4)^2 = 10^8$ order of magnitude (due to one high-dimensional matrix) to $10^3 \times 10^2 = 10^5$ (a thousand of small matrices). In our applicative context, the strategy of dividing a big problem into independent smaller ones appears beneficial from both the applicative and statistical perspective.

This being said, the question of the *global* inference, in contrast with a peptide-by-peptide approach, remains pregnant. To illustrate this topic, let us provide on Figure 7 an example of simultaneous differential analysis for nine peptides from the same protein. According to our previous recommendations, we accounted for the correlations through the multivariate algorithm and displayed the results in posterior mean's differences for each peptide from the P12081ups|SYHC_HUMAN_UPS protein at once (*i.e.* $\mu_1 - \mu_7$). In this example, eight peptides over nine contained in the protein are clearly differential in the same direction with comparable effect sizes, corroborating our intuition of correlated quantities. However, the situation may become far trickier when distributions lie closer to 0 on the x-axis or if only one peptide presents a clear differential pattern. As multiple and heterogeneous situations could be encountered, we do not provide recommendations here for directly dealing with protein-scale inference. Once again, the criterion for deciding what should be considered as *different enough* is highly dependent on the context and reasonable hypotheses, and no arbitrary threshold may bear any kind of general relevancy. However, we should still point out that our Bayesian framework provides convenient and natural interpretations in terms of probability for each peptide individually. It is then straightforward to construct probabilistic decision rules and combine them to reach a multivariate inference tool, for instance, by computing an average probability for the means' difference to be below 0 across all peptides. However, one should note that probability rules prevent directly deriving global probabilistic statements without closely looking at dependencies between the single events (for instance, the factorisation in Equation (3) holds thanks to the induced independence between peptides). Although such an automatic procedure cannot replace expert analysis, it may still provide a handy tool for extracting the most noteworthy results from a massive number of comparisons, which the practitioner should look at more closely afterwards. Therefore, once a maximal risk of the adverse event or a minimum probability of the desired outcome has been defined, one may derive the adequate procedure to reach those properties.

4 Conclusion and perspectives

This article presents a Bayesian inference framework to tackle the problem of differential analysis in both univariate and multivariate contexts while accounting for possible missing data. We proposed two algorithms, leveraging classical results from conjugate priors to compute posterior distributions and

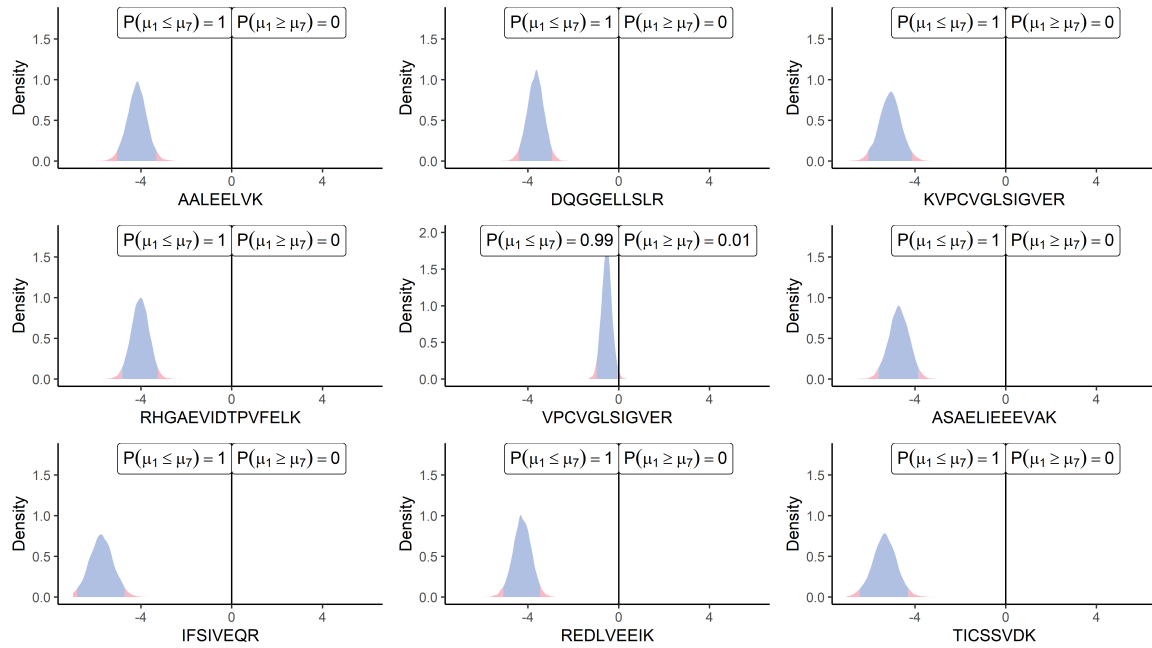


Figure 7: Posterior distributions of mean difference $\mu_1 - \mu_7$ for the nine peptides from the P12081ups|SYHC_HUMAN_UPS protein using the multivariate approach.

easily sample the difference of means when comparing groups of interest. For handling the recurrent problem of missing data, our multivariate approach takes advantage of the multiple imputations' approximation, while the univariate framework allows us to merely ignore this issue. In addition, this methodology aims at providing information not only on the probability of the means' difference to be null but also on the uncertainty quantification as well as the effect sizes, which are crucial in a biological framework.

We believe that such probabilistic statements offer valuable inference tools to practitioners. In the particular context of differential proteomics, this methodology allows us to account for between-peptides correlations. With an adequate decision rule and an appropriate correlation structure, Bayesian inference could be used in large-scale proteomics experiments, such as label-free global quantification strategies. Nevertheless, targeted proteomics experiments could already benefit from this approach, as the set of considered peptides is restricted. Furthermore, such experiments used in biomarker research could greatly benefit from the quantification of the uncertainty and the assessment of the effect sizes.

5 Code availability

The work described in the present article was implemented as an R package called *ProteBayes*, available on CRAN, while a development version can be found on GitHub (github.com/mariechion/ProteoBayes). A web app has also been developed and can be accessed at arthurleroy.shinyapps.io/ProteoBayes.

6 Data availability

The *Arabidopsis thaliana* spiked dataset is public and accessible on the ProteomeXchange website using the PXD027800 identifier.

7 Proofs

7.1 Proof of Bayesian inference for Normal-Inverse-Gamma conjugated priors

Let us recall below the complete development of this derivation by identification of the analytical form (we ignore conditioning over the hyper-parameters for convenience):

$$\begin{aligned}
p(\mu, \sigma^2 \mid \mathbf{y}) &\propto p(\mathbf{y} \mid \mu, \sigma^2) \times p(\mu, \sigma^2) \\
&= \left(\frac{1}{2\pi\sigma^2} \right)^{\frac{N}{2}} \exp \left(-\frac{1}{2\sigma^2} \sum_{n=1}^N (y_n - \mu)^2 \right) \\
&\quad \times \frac{\sqrt{\lambda_0}}{\sqrt{2\pi}} \frac{\beta_0^{\alpha_0}}{\Gamma(\alpha_0)} \left(\frac{1}{\sigma^2} \right)^{\alpha_0 + \frac{3}{2}} \exp \left(-\frac{2\beta_0 + \lambda_0(\mu - \mu_0)^2}{2\sigma^2} \right) \\
&\propto \left(\frac{1}{\sigma^2} \right)^{\alpha_0 + \frac{N+3}{2}} \exp \left(-\underbrace{\frac{2\beta_0 + \lambda_0(\mu - \mu_0)^2 + \sum_{n=1}^N (y_n - \mu)^2}{2\sigma^2}}_{\mathcal{A}} \right).
\end{aligned}$$

Let us introduce Lemma 1 below to decompose the term \mathcal{A} as desired:

Lemma 1. Assume a set $\mathbf{x}_1, \dots, \mathbf{x}_N \in \mathbb{R}^q$, and note $\bar{\mathbf{x}} = \frac{1}{N} \sum_{n=1}^N \mathbf{x}_n$ the associated average vector. For any $\boldsymbol{\mu} \in \mathbb{R}^q$:

$$\sum_{n=1}^N (\mathbf{x}_n - \boldsymbol{\mu})(\mathbf{x}_n - \boldsymbol{\mu})^\top = N(\bar{\mathbf{x}} - \boldsymbol{\mu})(\bar{\mathbf{x}} - \boldsymbol{\mu})^\top + \sum_{n=1}^N (\mathbf{x}_n - \bar{\mathbf{x}})(\mathbf{x}_n - \bar{\mathbf{x}})^\top.$$

Proof.

$$\begin{aligned}
\sum_{n=1}^N (\mathbf{x}_n - \boldsymbol{\mu})(\mathbf{x}_n - \boldsymbol{\mu})^\top &= \sum_{n=1}^N \mathbf{x}_n \mathbf{x}_n^\top + \boldsymbol{\mu} \boldsymbol{\mu}^\top - 2\mathbf{x}_n \boldsymbol{\mu}^\top \\
&= N\boldsymbol{\mu} \boldsymbol{\mu}^\top - 2N\bar{\mathbf{x}} \boldsymbol{\mu}^\top + \sum_{n=1}^N \mathbf{x}_n \mathbf{x}_n^\top \\
&= N\boldsymbol{\mu} \boldsymbol{\mu}^\top + N\bar{\mathbf{x}} \bar{\mathbf{x}}^\top + N\bar{\mathbf{x}} \bar{\mathbf{x}}^\top - 2N\bar{\mathbf{x}} \bar{\mathbf{x}}^\top - 2N\bar{\mathbf{x}} \boldsymbol{\mu}^\top + \sum_{n=1}^N \mathbf{x}_n \mathbf{x}_n^\top \\
&= N(\bar{\mathbf{x}} \bar{\mathbf{x}}^\top - \boldsymbol{\mu} \boldsymbol{\mu}^\top - 2\bar{\mathbf{x}} \boldsymbol{\mu}^\top) + \sum_{n=1}^N \mathbf{x}_n \mathbf{x}_n^\top + \bar{\mathbf{x}} \bar{\mathbf{x}}^\top - 2\mathbf{x}_n \bar{\mathbf{x}}^\top \\
&= N(\bar{\mathbf{x}} - \boldsymbol{\mu})(\bar{\mathbf{x}} - \boldsymbol{\mu})^\top + \sum_{n=1}^N (\mathbf{x}_n - \bar{\mathbf{x}})(\mathbf{x}_n - \bar{\mathbf{x}})^\top.
\end{aligned}$$

□

Applying this result in our context for $q = 1$, we obtain:

$$\begin{aligned}
\mathcal{A} &= -\frac{1}{2\sigma^2} \left(2\beta_0 + \lambda_0(\mu - \mu_0)^2 + N(\bar{y} - \mu)^2 + \sum_{n=1}^N (y_n - \bar{y})^2 \right) \\
&= -\frac{1}{2\sigma^2} \left(2\beta_0 + \sum_{n=1}^N (y_n - \bar{y})^2 + (\lambda_0 + N)\mu^2 - 2\mu(N\bar{y} + \lambda_0\mu_0) + N\bar{y}^2 + \lambda_0\mu_0^2 \right) \\
&= -\frac{1}{2\sigma^2} \left(2\beta_0 + \sum_{n=1}^N (y_n - \bar{y})^2 + N\bar{y}^2 + \lambda_0\mu_0^2 \right)
\end{aligned}$$

$$\begin{aligned}
& + (\lambda_0 + N) \left[\mu^2 - 2\mu \frac{N\bar{y} + \lambda_0\mu_0}{\lambda_0 + N} + \left(\frac{N\bar{y} + \lambda_0\mu_0}{\lambda_0 + N} \right)^2 - \left(\frac{N\bar{y} + \lambda_0\mu_0}{\lambda_0 + N} \right)^2 \right] \\
& = -\frac{1}{2\sigma^2} \left(2\beta_0 + \sum_{n=1}^N (y_n - \bar{y})^2 + N\bar{y}^2 + \lambda_0\mu_0^2 - \frac{(N\bar{y} + \lambda_0\mu_0)^2}{\lambda_0 + N} \right. \\
& \quad \left. + (\lambda_0 + N) \left(\mu - \frac{N\bar{y} + \lambda_0\mu_0}{\lambda_0 + N} \right)^2 \right) \\
& = -\frac{1}{2\sigma^2} \left(2\beta_0 + \sum_{n=1}^N (y_n - \bar{y})^2 + \frac{(\lambda_0 + N)(N\bar{y}^2 + \lambda_0\mu_0^2) - N^2\bar{y}^2 - \lambda_0^2\mu_0^2 + 2N\bar{y}\lambda_0\mu_0}{\lambda_0 + N} \right. \\
& \quad \left. + (\lambda_0 + N) \left(\mu - \frac{N\bar{y} + \lambda_0\mu_0}{\lambda_0 + N} \right)^2 \right) \\
& = -\frac{1}{2\sigma^2} \left(2\beta_0 + \sum_{n=1}^N (y_n - \bar{y})^2 + \frac{\lambda_0 N}{\lambda_0 + N} (\bar{y} - \mu_0)^2 + (\lambda_0 + N) \left(\mu - \frac{N\bar{y} + \lambda_0\mu_0}{\lambda_0 + N} \right)^2 \right).
\end{aligned}$$

7.2 Proof of General Bayesian framework for evaluating mean differences

Proof. For the sake of clarity, let us omit the K groups here and first consider a general case with $\mathbf{y}_k = \mathbf{y} \in \mathbb{R}^P$. Moreover, let us focus on only one imputed dataset and maintain the notation $\tilde{\mathbf{y}}_1^{(d)}, \dots, \tilde{\mathbf{y}}_N^{(d)} = \mathbf{y}_1, \dots, \mathbf{y}_N$ for convenience. From the hypotheses of the model, we can derive \mathcal{L} , the posterior log-PDF over $(\boldsymbol{\mu}, \boldsymbol{\Sigma})$, following the same idea as for the univariate case presented in Section 2.1:

$$\begin{aligned}
\mathcal{L} & = \log p(\boldsymbol{\mu}, \boldsymbol{\Sigma} \mid \mathbf{y}_1, \dots, \mathbf{y}_N) \\
& = \log \underbrace{p(\mathbf{y}_1, \dots, \mathbf{y}_N \mid \boldsymbol{\mu}, \boldsymbol{\Sigma})}_{\mathcal{N}(\boldsymbol{\mu}, \boldsymbol{\Sigma})} + \log \underbrace{p(\boldsymbol{\mu}, \boldsymbol{\Sigma})}_{\mathcal{N}\mathcal{W}^{-1}(\boldsymbol{\mu}_0, \lambda_0, \boldsymbol{\Sigma}_0, \nu_0)} + C_1 \\
& = -\frac{N}{2} \log |\boldsymbol{\Sigma}| - \frac{1}{2} \left(\sum_{n=1}^N (\mathbf{y}_n - \boldsymbol{\mu})^\top \boldsymbol{\Sigma}^{-1} (\mathbf{y}_n - \boldsymbol{\mu}) \right) \\
& \quad - \frac{\nu_0 + P + 2}{2} \log |\boldsymbol{\Sigma}| - \frac{1}{2} \left(\text{tr}(\boldsymbol{\Sigma}_0 \boldsymbol{\Sigma}^{-1}) - \frac{\lambda_0}{2} (\boldsymbol{\mu} - \boldsymbol{\mu}_0)^\top \boldsymbol{\Sigma}^{-1} (\boldsymbol{\mu} - \boldsymbol{\mu}_0) \right) + C_2 \\
& = -\frac{1}{2} \left[(\nu_0 + P + 2 + N) \log |\boldsymbol{\Sigma}| + \text{tr}(\boldsymbol{\Sigma}_0 \boldsymbol{\Sigma}^{-1}) \right. \\
& \quad \left. + \sum_{n=1}^N \text{tr}((\mathbf{y}_n - \boldsymbol{\mu})^\top \boldsymbol{\Sigma}^{-1} (\mathbf{y}_n - \boldsymbol{\mu})) + \text{tr}(\lambda_0 (\boldsymbol{\mu} - \boldsymbol{\mu}_0)^\top \boldsymbol{\Sigma}^{-1} (\boldsymbol{\mu} - \boldsymbol{\mu}_0)) \right] + C_2 \\
& = -\frac{1}{2} \left[(\nu_0 + P + 2 + N) \log |\boldsymbol{\Sigma}| + \text{tr} \left(\boldsymbol{\Sigma}^{-1} \left\{ \boldsymbol{\Sigma}_0 + \lambda_0 (\boldsymbol{\mu} - \boldsymbol{\mu}_0) (\boldsymbol{\mu} - \boldsymbol{\mu}_0)^\top \right. \right. \right. \\
& \quad \left. \left. \left. + \underbrace{N(\bar{\mathbf{y}} - \boldsymbol{\mu})(\bar{\mathbf{y}} - \boldsymbol{\mu})^\top + \sum_{n=1}^N (\mathbf{y}_n - \bar{\mathbf{y}})(\mathbf{y}_n - \bar{\mathbf{y}})^\top}_{\text{Lemma 1}} \right\} \right) \right] + C_2 \\
& = -\frac{1}{2} \left[(\nu_0 + P + 2 + N) \log |\boldsymbol{\Sigma}| + \text{tr} \left(\boldsymbol{\Sigma}^{-1} \left\{ \boldsymbol{\Sigma}_0 + \sum_{n=1}^N (\mathbf{y}_n - \bar{\mathbf{y}})(\mathbf{y}_n - \bar{\mathbf{y}})^\top \right. \right. \right. \\
& \quad \left. \left. \left. + (N + \lambda_0) \boldsymbol{\mu} \boldsymbol{\mu}^\top - \boldsymbol{\mu} (N\bar{\mathbf{y}}^\top + \lambda_0 \boldsymbol{\mu}_0^\top) - (\lambda_0 \boldsymbol{\mu}_0 + N\bar{\mathbf{y}}) \boldsymbol{\mu}^\top + \lambda_0 \boldsymbol{\mu}_0 \boldsymbol{\mu}_0^\top + N\bar{\mathbf{y}} \bar{\mathbf{y}}^\top \right\} \right) \right] + C_2 \\
& = -\frac{1}{2} \left[(\nu_0 + P + 2 + N) \log |\boldsymbol{\Sigma}| \right.
\end{aligned}$$

$$\begin{aligned}
& + \text{tr} \left(\boldsymbol{\Sigma}^{-1} \left\{ \boldsymbol{\Sigma}_0 + \sum_{n=1}^N (\mathbf{y}_n - \bar{\mathbf{y}})(\mathbf{y}_n - \bar{\mathbf{y}})^\top + \frac{N\lambda_0}{N + \lambda_0} (\bar{\mathbf{y}} - \boldsymbol{\mu}_0)(\bar{\mathbf{y}} - \boldsymbol{\mu}_0)^\top \right. \right. \\
& \left. \left. + (N + \lambda_0) \left(\boldsymbol{\mu} - \frac{N\bar{\mathbf{y}} + \lambda_0\boldsymbol{\mu}_0}{N + \lambda_0} \right) \left(\boldsymbol{\mu} - \frac{N\bar{\mathbf{y}} + \lambda_0\boldsymbol{\mu}_0}{N + \lambda_0} \right)^\top \right\} \right) + C_2 \\
& = -\frac{1}{2} \left[(\nu_N + P + 2) \log |\boldsymbol{\Sigma}| + \text{tr} (\boldsymbol{\Sigma}^{-1} \boldsymbol{\Sigma}_N) + \lambda_N (\boldsymbol{\mu} - \boldsymbol{\mu}_N)^\top \boldsymbol{\Sigma}^{-1} (\boldsymbol{\mu} - \boldsymbol{\mu}_N) \right] + C_2.
\end{aligned}$$

By identification, we recognise the log-PDF that characterises the Gaussian-inverse-Wishart distribution $\mathcal{NIW}^{-1}(\boldsymbol{\mu}_N, \lambda_N, \boldsymbol{\Sigma}_N, \nu_N)$ with:

- $\boldsymbol{\mu}_N = \frac{N\bar{\mathbf{y}} + \lambda_0\boldsymbol{\mu}_0}{N + \lambda_0}$,
- $\lambda_N = \lambda_0 + N$,
- $\boldsymbol{\Sigma}_N = \boldsymbol{\Sigma}_0 + \sum_{n=1}^N (\mathbf{y}_n - \bar{\mathbf{y}})(\mathbf{y}_n - \bar{\mathbf{y}})^\top + \frac{\lambda_0 N}{(\lambda_0 + N)} (\bar{\mathbf{y}} - \boldsymbol{\mu}_0)(\bar{\mathbf{y}} - \boldsymbol{\mu}_0)^\top$,
- $\nu_N = \nu_0 + N$.

Once more, we can integrate over $\boldsymbol{\Sigma}$ to compute the mean's marginal posterior distribution by identifying the PDF of the inverse-Wishart distribution $\mathcal{W}^{-1}(\boldsymbol{\Sigma}_N + \lambda_N (\boldsymbol{\mu} - \boldsymbol{\mu}_N)(\boldsymbol{\mu} - \boldsymbol{\mu}_N)^\top, \nu_N + 1)$ and by reorganising the terms:

$$\begin{aligned}
p(\boldsymbol{\mu} | \mathbf{y}) & = \int p(\boldsymbol{\mu}, \boldsymbol{\Sigma} | \mathbf{y}) d\boldsymbol{\Sigma} \\
& = \frac{\lambda_N^{\frac{P}{2}} |\boldsymbol{\Sigma}_N|^{\frac{\nu_N}{2}}}{(2\pi)^{\frac{P}{2}} 2^{\frac{P\nu_N}{2}} \Gamma_P\left(\frac{\nu_N}{2}\right)} \\
& \quad \times \int |\boldsymbol{\Sigma}|^{-\frac{\nu_N + P + 2}{2}} \exp\left(-\frac{1}{2} \left(\text{tr} (\boldsymbol{\Sigma}_N \boldsymbol{\Sigma}^{-1}) - \frac{\lambda_N}{2} (\boldsymbol{\mu} - \boldsymbol{\mu}_N)^\top \boldsymbol{\Sigma}^{-1} (\boldsymbol{\mu} - \boldsymbol{\mu}_N) \right)\right) d\boldsymbol{\Sigma} \\
& = \frac{\lambda_N^{\frac{P}{2}} |\boldsymbol{\Sigma}_N|^{\frac{\nu_N}{2}}}{(2\pi)^{\frac{P}{2}} 2^{\frac{P\nu_N}{2}} \Gamma_P\left(\frac{\nu_N}{2}\right)} \times \frac{2^{\frac{P(\nu_N + 1)}{2}} \Gamma_P\left(\frac{\nu_N + 1}{2}\right)}{|\boldsymbol{\Sigma}_N + \lambda_N (\boldsymbol{\mu} - \boldsymbol{\mu}_N)(\boldsymbol{\mu} - \boldsymbol{\mu}_N)^\top|^{\frac{\nu_N + 1}{2}}} \times 1 \\
& = \frac{\pi^{p(p-1)/4} \prod_{p=0}^{P-1} \Gamma\left(\frac{\nu_N + 1 - p}{2}\right)}{\pi^{P(P-1)/4} \prod_{p=1}^P \Gamma\left(\frac{\nu_N + 1 - p}{2}\right)} \times \frac{\lambda_N^{\frac{P}{2}}}{\pi^{\frac{P}{2}}} \\
& \quad \times \underbrace{\frac{|\boldsymbol{\Sigma}_N|^{\frac{\nu_N}{2}}}{|\boldsymbol{\Sigma}_N|^{\frac{\nu_N + 1}{2}}} \times (1 + \lambda_N (\boldsymbol{\mu} - \boldsymbol{\mu}_N)^\top \boldsymbol{\Sigma}_N^{-1} (\boldsymbol{\mu} - \boldsymbol{\mu}_N))^{-\frac{\nu_N + 1}{2}}}_{\text{Matrix determinant lemma}} \\
& = \frac{\Gamma\left(\frac{\nu_N + 1}{2}\right)}{\Gamma\left(\frac{\nu_N + 1 - P}{2}\right)} \times \frac{[\lambda_N(\nu_N - P + 1)]^{\frac{P}{2}}}{[\pi(\nu_N - P + 1)]^{\frac{P}{2}} |\boldsymbol{\Sigma}_N|^{\frac{1}{2}}} \\
& \quad \times \left(1 + \frac{\lambda_N(\nu_N - P + 1)}{(\nu_N - P + 1)} (\boldsymbol{\mu} - \boldsymbol{\mu}_N)^\top \boldsymbol{\Sigma}_N^{-1} (\boldsymbol{\mu} - \boldsymbol{\mu}_N) \right)^{-\frac{\nu_N + 1}{2}} \\
& = \frac{\Gamma\left(\frac{(\nu_N - P + 1) + P}{2}\right)}{\Gamma\left(\frac{\nu_N - P + 1}{2}\right) [\pi(\nu_N - P + 1)]^{\frac{P}{2}} \left| \frac{\boldsymbol{\Sigma}_N}{\lambda_N(\nu_N - P + 1)} \right|^{\frac{1}{2}}} \\
& \quad \times \left(1 + \frac{1}{\nu_N - P + 1} (\boldsymbol{\mu} - \boldsymbol{\mu}_N)^\top \left(\frac{\boldsymbol{\Sigma}_N}{\lambda_N(\nu_N - P + 1)} \right)^{-1} (\boldsymbol{\mu} - \boldsymbol{\mu}_N) \right)^{-\frac{(\nu_N - P + 1) + P}{2}}.
\end{aligned}$$

The above expression corresponds to the PDF of a multivariate t -distribution $\mathcal{T}_\nu(\boldsymbol{\mu}_N, \hat{\boldsymbol{\Sigma}})$, with:

- $\nu = \nu_N - P + 1$,
- $\hat{\boldsymbol{\Sigma}} = \frac{\boldsymbol{\Sigma}_N}{\lambda_N(\nu_N - P + 1)}$.

Therefore, we demonstrated that for each group and imputed dataset, the complete-data posterior distribution over $\boldsymbol{\mu}_k$ is a multivariate t -distribution. Thus, following Rubin’s rules for multiple imputation (see (Little and Rubin, 2019)), we can propose an approximation to the true posterior distribution (that is only conditioned over observed values):

$$\begin{aligned} p(\boldsymbol{\mu}_k | \mathbf{y}_k^{(0)}) &= \int p(\boldsymbol{\mu}_k | \mathbf{y}_k^{(0)}, \mathbf{y}_k^{(1)}) p(\mathbf{y}_k^{(1)} | \mathbf{y}_k^{(0)}) d\mathbf{y}_k^{(1)} \\ &\simeq \frac{1}{P} \sum_{p=1}^P p(\boldsymbol{\mu}_k | \mathbf{y}_k^{(0)}, \tilde{\mathbf{y}}_k^{(1),d}) \end{aligned}$$

Leading to the desired results when evaluating the previously derived posterior distribution on each multiple-imputed dataset. \square

References

- Constantin Ahlmann-Eltze and Simon Anders. proDA: Probabilistic Dropout Analysis for Identifying Differentially Abundant Proteins in Label-Free Mass Spectrometry, May 2020.
- Rebecca A. Betensky. The p-Value Requires Context, Not a Threshold. *The American Statistician*, 73(sup1):115–117, March 2019. ISSN 0003-1305. doi: 10.1080/00031305.2018.1529624.
- Christopher M. Bishop. *Pattern Recognition and Machine Learning*. Springer, August 2006. ISBN 978-0-387-31073-2.
- Cheng Chang, Kaikun Xu, Chaoping Guo, Jinxia Wang, Qi Yan, Jian Zhang, Fuchu He, and Yunping Zhu. PANDA-view: An easy-to-use tool for statistical analysis and visualization of quantitative proteomics data. *Bioinformatics*, 34(20):3594–3596, October 2018. ISSN 1367-4803. doi: 10.1093/bioinformatics/bty408.
- Marie Chion, Christine Carapito, and Frédéric Bertrand. Accounting for multiple imputation-induced variability for differential analysis in mass spectrometry-based label-free quantitative proteomics. *PLOS Computational Biology*, 18(8):e1010420, August 2022. ISSN 1553-7358. doi: 10.1371/journal.pcbi.1010420.
- Meena Choi, Ching-Yun Chang, Timothy Clough, Daniel Broudy, Trevor Killeen, Brendan MacLean, and Olga Vitek. MSstats: An R package for statistical analysis of quantitative mass spectrometry-based proteomic experiments. *Bioinformatics*, 30(17):2524–2526, September 2014. ISSN 1367-4803. doi: 10.1093/bioinformatics/btu305.
- Oliver M. Crook, Chun-wa Chung, and Charlotte M. Deane. Challenges and Opportunities for Bayesian Statistics in Proteomics. *Journal of Proteome Research*, 21(4):849–864, April 2022. ISSN 1535-3893. doi: 10.1021/acs.jproteome.1c00859.
- Francesca Dominici, Giovanni Parmigiani, and Merlise Clyde. Conjugate Analysis of Multivariate Normal Data with Incomplete Observations. *The Canadian Journal of Statistics / La Revue Canadienne de Statistique*, 28(3):533–550, 2000. ISSN 0319-5724. doi: 10.2307/3315963.
- John K. Kruschke. Bayesian estimation supersedes the t test. *Journal of Experimental Psychology. General*, 142(2):573–603, May 2013. ISSN 1939-2222. doi: 10.1037/a0029146.
- John K. Kruschke and Torrin M. Liddell. The Bayesian New Statistics: Hypothesis testing, estimation, meta-analysis, and power analysis from a Bayesian perspective. *Psychonomic Bulletin & Review*, 25(1):178–206, February 2018. ISSN 1531-5320. doi: 10.3758/s13423-016-1221-4.

- Cosmin Lazar, Laurent Gatto, Myriam Ferro, Christophe Bruley, and Thomas Burger. Accounting for the Multiple Natures of Missing Values in Label-Free Quantitative Proteomics Data Sets to Compare Imputation Strategies. *Journal of Proteome Research*, 15(4):1116–1125, April 2016. ISSN 1535-3893. doi: 10.1021/acs.jproteome.5b00981.
- Roderick JA Little and Donald B Rubin. *Statistical analysis with missing data*, volume 793. John Wiley & Sons, 2019.
- Kevin P Murphy. Conjugate bayesian analysis of the gaussian distribution. *def*, 1(2 σ 2):16, 2007.
- Jonathon J. O’Brien, Harsha P. Gunawardena, Joao A. Paulo, Xian Chen, Joseph G. Ibrahim, Steven P. Gygi, and Bahjat F. Qaqish. The effects of nonignorable missing data on label-free mass spectrometry proteomics experiments. *Annals of Applied Statistics*, 12(4):2075–2095, December 2018. ISSN 1932-6157, 1941-7330. doi: 10.1214/18-AOAS1144.
- Gordon K Smyth. Linear Models and Empirical Bayes Methods for Assessing Differential Expression in Microarray Experiments. *Statistical Applications in Genetics and Molecular Biology*, 3(1):1–25, January 2004. ISSN 1544-6115. doi: 10.2202/1544-6115.1027.
- Gail M. Sullivan and Richard Feinn. Using Effect Size—or Why the P Value Is Not Enough. *Journal of Graduate Medical Education*, 4(3):279–282, September 2012. ISSN 1949-8349. doi: 10.4300/JGME-D-12-00156.1.
- Matthew The and Lukas Käll. Integrated Identification and Quantification Error Probabilities for Shotgun Proteomics * [S]. *Molecular & Cellular Proteomics*, 18(3):561–570, March 2019. ISSN 1535-9476, 1535-9484. doi: 10.1074/mcp.RA118.001018.
- Stefka Tyanova, Tikira Temu, Pavel Sinitcyn, Arthur Carlson, Marco Y Hein, Tamar Geiger, Matthias Mann, and Jürgen Cox. The Perseus computational platform for comprehensive analysis of (prote)omics data. *Nature Methods*, 13(9):731–740, September 2016. ISSN 1548-7091, 1548-7105. doi: 10.1038/nmeth.3901.
- Ronald L. Wasserstein, Allen L. Schirm, and Nicole A. Lazar. Moving to a World Beyond “ $p < 0.05$ ”. *The American Statistician*, 73(sup1):1–19, March 2019. ISSN 0003-1305. doi: 10.1080/00031305.2019.1583913.
- Samuel Wiczorek, Florence Combes, Cosmin Lazar, Quentin Gai Gianetto, Laurent Gatto, Alexia Dorffer, Anne-Marie Hesse, Yohann Couté, Myriam Ferro, Christophe Bruley, and Thomas Burger. DAPAR & ProStaR: Software to perform statistical analyses in quantitative discovery proteomics. *Bioinformatics (Oxford, England)*, 33(1):135–136, January 2017. ISSN 1367-4811. doi: 10.1093/bioinformatics/btw580.